Multi-Modality Imaging of Bone Marrow Edema-Like Lesions and Associated Cartilage in Osteoarthritic Patients

D. Kuo[1], J. Schooler[1], J. Goldenstein[1], S. Siddiqui[1], S. Shanbhag[1], J-B. Pialat[1], A. Burghardt[1], S. Majumdar[1], M. Ries[2], G. Kazakia[1], and X. Li[1]
[1]Musculoskeletal Quantitative Imaging Research (MQIR), Department of Radiology and Biomedical Imaging, University of California, San Francisco, San Francisco, CA, United States, [2]Department of Orthopaedic Surgery, University of California, San Francisco, San Francisco, CA, United States

INTRODUCTION

Osteoarthritis (OA) is a complex disease that affects not only cartilage but bone as well. Bone marrow edema-like lesions (BMEL), identified as diffuse regions of high signal on T2-weighted fat saturated magnetic resonance (MR) images, are commonly seen in OA. They have been correlated with OA progression and pain (1,2). However, knowledge of their natural history, relation to cartilage change, and underlying bone structure is limited. Previous studies have shown that biochemical cartilage matrix changes can be detected prior to morphological changes using advanced MR $T_{1\rho}$ and T_2 mapping techniques (3). Therefore, in this study, we examined cartilage associated with BMEL by quantifying MR $T_{1\rho}$ and T_2 relaxation times and evaluated bone structure and composition of BMEL using high resolution peripheral quantitative computed tomography (HR-pQCT) imaging and Fourier transform infrared (FTIR) spectroscopy.

METHODS

Eleven tibial plateau specimens containing cartilage and subchondral bone were collected from severe OA patients who had total knee replacement. Specimens were glued to a plastic grid for location references and registration landmarks, immersed in lactated Ringer's solution, and then imaged with MRI (Signa 3T, GE) using a transmit/receive 8-channel knee coil. The protocol included sagittal, T2-weighted fat-saturated fast spin-echo (FSE) images to identify BMEL (TR/TE = 4300/51 ms, field of view [FOV] = 10 cm, matrix size = 512x256, slice thickness = 1.5 mm, echo train length [ETL] = 9, bandwidth [BW] = 31.25 kHz, number of excitations [NEX] = 2), a 3D $T_{1\rho}$ quantification sequence we developed previously (in plane resolution = 0.4 mm, slice thickness = 2 mm, time of spin-lock [TSL] = 0, 10, 40, 80 ms, frequency of spin-lock [FSL] = 500 Hz), and a 3D T2 quantification sequence (TE = 3/14/25/46 ms, in plane resolution = 0.4 mm, slice thickness = 2 mm). Specimens with BMEL were then imaged with HR-pQCT (XtremeCT, Scanco Medical AG) using the standard manufacturer-suggested protocol (isotropic 41-μm voxels, source potential = 60 kVp, tube current = 900 μA, integration time = 100 ms). With FSE images as a guide, a 3mm slice containing BMEL was cut from each specimen, marrow was removed, and two 3 mm diameter punches were taken - one inside BMEL, the other outside BMEL. FTIR spectroscopy was performed on the punches using a benchtop interferometer system (Nexus 870, Thermo Electron) with spectra acquired using 256 scans at 4 cm^{-1} spectral resolution.

Thresholded BMEL contours were generated for FSE images using an in-house developed software. Cartilage was semi-automatically segmented in $T_{1\rho}$-weighted SPGR images with TSL = 0. The mean $T_{1\rho}$ and T_2 values were quantified in cartilage overlying BMEL and in surrounding cartilage. For bone structure data, MR images were registered to downsampled HR-pQCT images (Fig. 1) with a 3D rigid volume registration that uses normalized mutual information (Rview, C. Studholme). HR-pQCT images were binarized with an automated iterative thresholding scheme and then overlaid with upsampled BMEL contours. Bone structure parameters including bone volume fraction (BV/TV), trabecular thickness (Tb.Th), trabecular inhomogeneity (Tb.1/N.SD) and apparent density were quantified. Baseline-corrected FTIR spectra were used to determine integrated areas of the collagen amide I (1600-1700 cm^{-1}) and phosphate (PO_4, 900-1200 cm^{-1}) bands. Mineral-to-matrix ratio (PO4/amide I) was calculated. Wilcoxon sign-rank tests for paired samples were conducted to assess differences between cartilage overlying and surrounding BMEL, as well as measures in BMEL and non-BMEL bone.

RESULTS

Nine out of 11 specimens had BMEL and went through the full protocol. Among the remaining 9 specimen, 5 had little to no cartilage overlying BMEL. In the 4 specimens with sufficient cartilage for analysis, we saw significantly elevated $T_{1\rho}$ and T_2 values in cartilage overlying BMEL (OC) versus surrounding cartilage (SC) ($T_{1\rho}$: 51.7 ± 8.1 ms in SC vs 60.5 ± 5.9 ms in OC, $P < 0.05$; T_2: 34.4 ± 0.3 in SC vs. 48.7 ± 16.7 in OC, $P < 0.05$). In all 9 specimens bone tissue within BMEL had significantly higher BV/TV (BMEL 0.43 ± 0.09, non-BMEL 0.35 ± 0.06, p = 0.03), Tb.Th (BMEL 0.27 ± 0.05 mm, non-BMEL 0.22 ± 0.04 mm, p = 0.04), Tb.1/N.SD (BMEL 0.18 ± 0.06 mm, non-BMEL 0.13 ± 0.06 mm, p = 0.01), and apparent density (BMEL 336 ± 96 mgHA/cc, non-BMEL 190 ± 86 mgHA/cc, p = 0.04) (Table 1). Bone tissue within BMEL also had significantly lower mineral-to-matrix ratio than the adjacent tissue (Table 1: BMEL 5.1 ± 0.7, non-BMEL 5.7 ± 0.3, p = 0.02).

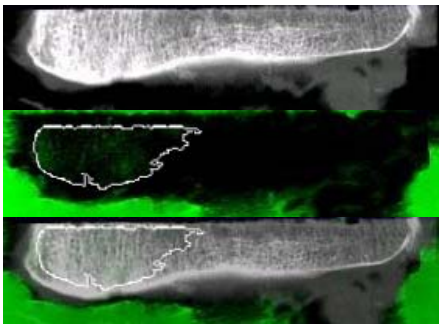

Table 1
Mean and SD of Bone Volume Fraction, Trabecular Thickness, Trabecular Inhomogeneity, Apparent Density, and Mineral-to-Matrix Ratio in BMEL and non-BMEL regions (N = 9)

	BV/TV	Tb.Th (mm)	Tb.T1/N.SD (mm)	Apparent Density (mmHA/cc)	Mineral-to-matrix ratio
BMEL	0.43 ± 0.09	0.27 ± 0.05	0.18 ± 0.06	336 ± 96	5.1 ± 0.7
Non-BMEL	0.35 ± 0.06	0.22 ± 0.04	0.13 ± 0.06	190 ± 86	5.7 ± 0.03

$P < 0.05$ between BMEL and Non-BMEL regions for each measure above.

Figure 1. Multi-modality registration of MR to HR-pQCT images. Downsampled HR-pQCT image shown on top. FSE (MR) image with white BMEL contour shown in the middle. Registered images shown on bottom. BMEL contour overlay can then be used for analysis of HR-pQCT data.

DISCUSSION

Our results using quantitative $T_{1\rho}$ and T_2 MRI indicate that regions of BMEL are associated with more advanced cartilage degeneration. Registering MR and HR-pQCT images, we observed increased bone volume and trabecular thickness within BMEL measured by HR-pQCT, which is consistent with a recent study using micro-CT (4). Bone tissue within BMEL also exhibited a greater degree of heterogeneity, indicating possible abnormal remodeling. Interestingly, we also observed reduced tissue mineralization within BMEL using FTIR. The fact that these changes exist within the BMEL regions but not in adjacent regions (also from an osteoarthritic joint) imply a localized imbalance in bone formation and mineralization specific to the BMEL region. These results suggest that BMEL may be involved in bone degeneration and therefore may be a therapeutic target and prognostic marker of OA progression. Advanced multi-modality imaging with MRI, HR-pQCT and FTIR provides quantitative assessment of BMEL and associated cartilage and bone degeneration.

REFERENCES

1. Felson D, et al., Ann Intern Med, 2003. 139 (Pt 1): 330-6.
2. Felson D, et al., Ann Intern Med, 2001. 134: 541-9.
3. Li et al, Osteoarthritis Cartilage, 2007.
4. Hunter et al, Arthritis Res Ther, 2009.

AKNOWLEDGEMENTS: This research was supported by UCSF Radiology tissue pilot funding. The authors would like to thank Eric Han from GE Healthcare for his help with sequence development, and Dr. Christoph Stehling for reviewing MRI images.